Internal H-C-C Angle Dependence of Vicinal ^1H-^1H Coupling Constants

Michael Barfield*,† and William B. Smith‡

Contribution from the Departments of Chemistry, University of Arizona, Tucson, Arizona 85721, and Texas Christian University, Fort Worth, Texas 76129. *Received July 22, 1991*

Abstract: Based on simple molecular orbital theory, an explicit expression is derived for vicinal H-H coupling constants $^3J_{HH'}(\theta_1,\theta_2,\phi)$ in terms of the two internal H-C-C angles θ_1 and θ_2 and the torsion angle ϕ: $^3J_{HH'}(\theta_1,\theta_2,\phi) = c_a\, a(\theta_1,\theta_2) \cos^2 \phi + \sum_i c_{bi}\, b_i(\theta_1,\theta_2) \cos \phi + C$. Important effects of both internal and torsion angle changes arise from the first term, where $a(\theta_1,\theta_2) = (1 + \cos \theta_1)(1 + \cos \theta_2)$, which decreases monotonically with increasing θ_1 and θ_2. The cos ϕ term has a more complicated dependence on internal angles. Since this term changes sign for $\phi = 90°$, the θ dependencies can be exceedingly different for $\phi < 90°$ than for $\phi > 90°$. Vicinal H-H coupling constants in ethanic moieties provide examples in which there is relatively little dependence on internal angles for $\phi < 90°$. The coefficients in the expression for $^3J_{HH'}(\theta_1,\theta_2,\phi)$ depend on the C-C internuclear distances and effective nuclear charges. These are determined empirically from the relatively few examples of vicinal H-H coupling which have been measured in rigid, unsubstituted molecules and from structural data obtained from either ab initio molecular orbital or molecular mechanics calculations. The resulting expressions provide excellent correlations of most features of vicinal H-H coupling in ethanic (CHCH), ethylenic (CH=CH), allylic (C=CHCH), and diene (C=CHCH=C) moieties and provide criteria for assessing the importance of internal angle changes.

Introduction

Because of their sensitivity to variations of *dihedral angles*,[1,2] vicinal H-H nuclear spin-spin coupling constants $^3J_{HH'}$ have been used extensively for conformational studies.[3,4] Factors such as H-C-C internal angle dependence, C-C bond length dependence, and substituent electronegativity are also involved.[5] The importance of changes in H-C-C angles was estimated by means of semiempirical valence-bond computations for an ethanic (CHCH) fragment with internal angles close to the tetrahedral value and for ethylenic fragments (CH=CH) at H-C-C angles of 115, 120, and 125°. In ethylenic systems for which the torsion angles are invariably fixed, the importance of H—C=C angle variations on $^3J_{HH'}$ was quickly recognized experimentally and studied extensively along with the roles of bond orders and C-C internuclear separation.[6-11]

For ethanic coupling there appears to have been no systematic investigation in which both the torsion angles and internal C-C-H angles are varied. Empirical studies[12-19] of ethanic coupling typically do not include internal angle changes, e.g., θ_1 and θ_2 angles in Figure 1 even though the VB results[5] indicated changes of several hertz if the θ angles varied by more than a few degrees from the tetrahedral value. Substantial deviations of internal H-C-C angles from the tetrahedral values are common in strained, multicyclic compounds. Because of their relative rigidity, such compounds are most appropriate for unambiguously relating spin-spin coupling constants to molecular structures. However, in ethanic systems one of the few obvious examples showing the importance of internal angle change is provided by the cubane molecule which has C-C-H angles near 125° and a cis H-H coupling constant of about 5.3 Hz.[20] This is just about half of the value expected in unstrained molecules.

Because of the importance of ethanic H-H coupling for organic stereochemistry,[12] much effort has been expended in specifying parameters for the torsion angle dependence especially the effects of substituent electronegativity.[12-14] Subsequent efforts have identified other factors, including substituent orientation[13-17] and electronic contributions to $^3J_{HH'}$ from other groups in the molecule, to account for the nonequivalence of the exo-exo and endo-endo vicinal coupling constants in bicyclo[2.2.1]heptanes.[21-23]

In contrast to the great interest in vicinal coupling in ethanic and ethylenic moieties, there have been few studies of vicinal coupling over the C-C single bond in allylic (C=CHCH) situations.[24,25] An empirical expression for the torsion angle dependence was proposed by Garbisch,[24] but the role of internal angles in these situations has not been discussed. In contrast, vicinal interproton coupling over a conjugated single bond, e.g.,

† University of Arizona.
‡ Texas Christian University.

(1) Karplus, M. *J. Chem. Phys.* **1959**, *30*, 11.
(2) Conroy, H. *Advances in Organic Chemistry*; Interscience: New York, 1960; Vol. II, p 265.
(3) Bystrov, V. F. *Prog. Nucl. Magn. Reson. Spectrosc.* **1976**, *10*, 41.
(4) Marchand, A. P. *Applications of NMR Studies in Rigid Bicyclic Systems*, Verlag Chimie International: Deerfield Beach, FL, 1982.
(5) Karplus, M. *J. Am. Chem. Soc.* **1963**, *85*, 2870.
(6) (a) Smith, G. V.; Kriloff, H. *J. Am. Chem. Soc.* **1963**, *85*, 2014. (b) Laszlo, P.; Schleyer, P. v. R. *J. Am. Chem. Soc.* **1963**, *85*, 2017.
(7) (a) Cooper, M. A.; Manatt, S. L. *J. Am. Chem. Soc.* **1969**, *91*, 6325. (b) Cooper, M. A.; Manatt, S. L. *J. Am. Chem. Soc.* **1970**, *92*, 1605. (c) Cooper, M. A.; Manatt, S. L. *J. Am. Chem. Soc.* **1970**, *92*, 4646. (d) Cooper, M. A.; Manatt, S. L. *Org. Magn. Reson.* **1970**, *2*, 511.
(8) (a) Rummens, F. H. A. *Org. Magn. Reson.* **1970**, *2*, 351. (b) Rummens, F. H. A.; Kaslander, L. *Can. J. Spectrosc.* **1972**, *17*, 99. (c) Rummens, F. H. A.; Kaslander, L. *Can. J. Chem.* **1976**, *54*, 2884.
(9) Solkan, V. N.; Sergeyev, N. M. *Org. Magn. Reson.* **1974**, *6*, 200.
(10) Günther, H.; Jikeli, G. *Chem. Rev.* **1977**, *77*, 613.
(11) Günther, H.; Schmickler, H.; Günther, M.-E.; Cremer, D. *Org. Magn. Reson.* **1977**, *9*, 420.
(12) For yearly reviews of the extensive literature in this area, see, for example, the chapters on nuclear spin-spin coupling in: *Nuclear Magnetic Resonance*; Specialist Periodical Reports; The Chemical Society, Burlington House: London, 1990.
(13) Durette, P. L.; Horton, D. *Org. Magn. Reson.* **1971**, *3*, 417.
(14) (a) Booth, H. *Tetrahedron Lett.* **1965**, 411. (b) Pachler, K. G. R. *J. Magn. Reson.* **1972**, *8*, 183. (c) Pachler, K. G. R. *Tetrahedron* **1971**, *27*, 187. (d) Pachler, K. G. R. *J. Chem. Soc., Perkin Trans. 2* **1972**, 1936.
(15) (a) Haasnoot, C. A. G.; de Leeuw, F. A. A. M.; Altona, C. *Tetrahedron* **1980**, *36*, 2783. (b) de Leeuw, F. A. A. M.; Altona, C.; Kessler, H.; Bermel, W.; Friedrich, A.; Krack, G.; Hull, W. E. *J. Am. Chem. Soc.* **1983**, *105*, 2237. (c) Donders, L. A.; de Leeuw, F. A. A. M.; Altona, C. *Magn. Reson. Chem.* **1989**, *27*, 556. (d) Altona, C.; Ippel, J. H. W.; Hoekzema, A. J. A.; Erkelens, C.; Groesbeek, M.; Donders, L. A. *Magn. Reson. Chem.* **1989**, *27*, 564.
(16) (a) Jaime, C.; Ōsawa, E.; Takeuchi, Y.; Camps, P. *J. Org. Chem.* **1983**, *48*, 4514. (b) Imai, K.; Ōsawa, E. *Magn. Reson. Chem.* **1990**, *28*, 668.
(17) Colucci, W. J.; Jungk, S. J.; Gandour, R. *Magn. Reson. Chem.* **1985**, *23*, 335.
(18) (a) Lambert, J. B. *J. Am. Chem. Soc.* **1967**, *89*, 1836. (b) Buys, H. R. *Recl. Trav. Chim. Pays-Bas* **1969**, *88*, 1003. (c) Forrest, T. P. *J. Am. Chem. Soc.* **1975**, *97*, 2628.
(19) Braun, S.; Lüttke, W. *Chem. Ber.* **1976**, *109*, 320.
(20) Edward, J. T.; Farrell, P. G.; Langford, G. E. *J. Am. Chem. Soc.* **1976**, *98*, 3075.
(21) Marshall, J. L.; Walter, S. R.; Barfield, M.; Marchand, A. P.; Marchand, N. W.; Segre, A. L. *Tetrahedron* **1976**, *32*, 537-542.
(22) Jaworski, A.; Ekiel, I.; Shugar, D. *J. Am. Chem. Soc.* **1978**, *100*, 4357.
(23) de Leeuw, F. A. A. M.; van Beuzekom, A. A.; Altona, C. *J. Comput. Chem.* **1983**, *4*, 438.
(24) Garbisch, E. W., Jr. *J. Am. Chem. Soc.* **1964**, *86*, 5561.
(25) Georgiadis, M. P.; Couladouros, W. A.; Polissiou, M. G.; Filippakis, S. E.; Mentzafos, D.; Terzis, A. *J. Org. Chem.* **1982**, *47*, 3054.

0002-7863/92/1514-1574$03.00/0 © 1992 American Chemical Society

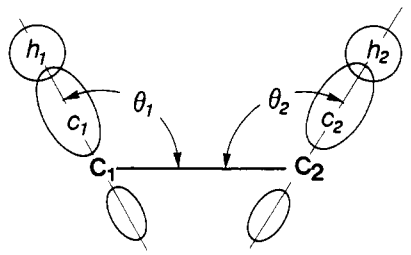

Figure 1. Schematic representation of a four-electron fragment of the ethane molecule. c_1 and c_2 denote the carbon hybrid orbitals directed toward the coupled hydrogen orbitals h_1 and h_2, respectively. The dihedral angle ϕ is measured about the C_1–C_2 bond, and the internal angles H_1–C_1–C_2 and C_1–C_2–H_2 are denoted θ_1 and θ_2, respectively.

the diene (C=CHCH=C) moiety, has been the subject of a number of investigations.[26-30] The increase of the vicinal coupling constant in a series of methyl-substituted butadienes and *all-trans*-retinal were empirically correlated with decreases in the C–C–H bond angles.[30]

An analytic expression for $^3J_{HH'}$ is derived and presented here to describe the dependence of vicinal H–H coupling constants on the internal angles θ_1 and θ_2, as well as the torsion angle ϕ. The coefficients in this expression, which are functions of the C–C internuclear distances and effective nuclear charges, were determined empirically for ethanic, ethylenic, allylic, and diene moieties, based primarily on data for strained cyclic molecules. The requisite geometrical data are optimized values from either ab initio MO calculations or molecular mechanics procedures.

Theoretical Discussion

The factors affecting vicinal coupling are examined using a simple molecular orbital (MO) description. An MO expression for the Fermi contact contribution to the spin–spin coupling constant $J_{NN'}$ between nuclei N and N′ was derived by Pople and Santry;[31] only the final result is given here

$$J_{NN'} = (4h)^{-1}(16\pi\beta\hbar/3)^2\,\gamma_N\gamma_{N'}\,s^2(N)\,s^2(N')\,\pi_{NN'} \quad (1)$$

where $s^2(N)$ and $s^2(N')$ denote the s-orbital densities at the coupled nuclei N and N′ and $\pi_{NN'}$ is the mutual atom–atom polarizability. Using this equation and an independent electron MO theory of hydrocarbons,[32] the same authors addressed the problems of geminal and vicinal ^1H–^1H and ^{13}C–^1H coupling in ethane, ethylene, and acetylene.[33] Perturbation theory was used to relate the mutual atom–atom polarizability in eq 1 to the various off-diagonal elements in the Hamiltonian matrix. For vicinal coupling this assumed a particularly simple form

$$\pi_{NN'} = \{-5\beta_{12}^2\}/(16\beta^3) \quad (2)$$

where β_{12} is the off-diagonal element of the Hamiltonian operator between hybrid type orbitals c_1 and c_2 in Figure 1. The off-diagonal element β in the denominator of eq 2 corresponds to an average of those between orbitals which are bonded in the primary valence structure. In semiempirical MO theory off-diagonal elements are simply assumed to be proportional to the corresponding overlap integrals. The integral β_{12} is the most important one for describing vicinal coupling. Numerical values for the integrals in eq 2 at tetrahedral and trigonal internal angles led to reasonable theoretical estimates of vicinal H–H coupling in ethane, ethylene, and acetylene.[33] Murrell and Gil[34] also used a perturbation approach but included the additional integrals which involve the hydrogens.

To obtain an expression for the off-diagonal element in the numerator of eq 2, consider a simple molecular orbital (MO) model[35] in which the MOs χ_i are written as a linear combination of hybrid (HTOs) and 1s-type orbitals on hydrogen

$$\chi_i = \sum_\mu c_{i\mu}\varphi_\mu \quad (3)$$

where the hybrid orbitals φ_μ can be written in terms of atomic s- and p-type atomic orbitals, the angle θ_μ that the hybrid orbital makes with the z-axis, and the dihedral angle ϕ about the z-axis[36]

$$\varphi_\mu = a_\mu s_\mu + (1 - a_\mu^2)^{1/2}[\cos\phi\,\sin\theta_\mu p_{x\mu} + \sin\phi\,\sin\theta_\mu p_{y\mu} + \cos\theta_\mu p_{\sigma\mu}] \quad (4)$$

where s_μ, $p_{x\mu}$, $p_{y\mu}$, and $p_{\sigma\mu}$ denote the 2s and 2p atomic orbitals associated with the μth hybrid orbital and a_μ is defined such that a_μ^2 is the s character of hybrid orbital μ. The overlap integral $S_{12} = \langle\varphi_1|\varphi_2\rangle$ between hybrid orbitals φ_1 and φ_2 which make respective angles θ_1 and θ_2 with the C–C bond and torsional angle ϕ with one another is

$$S_{12} = a_1a_2S_{ss} + (1 - a_1^2)^{1/2}(1 - a_2^2)^{1/2}\{\cos\phi\,\sin\theta_1\,\sin\theta_2\,S_{xx} + \cos\theta_1\,\cos\theta_2\,S_{\sigma\sigma}\} + \{a_1(1 - a_2^2)^{1/2}\cos\theta_2 + a_2(1 - a_1^2)^{1/2}\cos\theta_1\}S_{\sigma s} \quad (5)$$

where S_{ss}, for example, denotes the overlap integral between 2s atomic orbitals on C_1 and C_2. Analytic expressions are available for these integrals in terms of the internuclear separations $r(C_1$–$C_2)$ and the effective nuclear charges at the two carbon atoms.[37] The overlap integral between hybrid orbitals in eq 5 can be put in a more concise form

$$S_{12} = A'\cos\phi + B' \quad (6)$$

where A' and B' depend on the θ angles and the overlap integrals in eq 5. Because of the proportionality of β_{12} in eq 2 to the overlap integral in eq 6, $^3J_{HH'}$ is proportional to S_{12}^2

$$^3J_{HH'}(\theta_1,\theta_2,\phi) = K[A'^2\cos^2\phi + 2A'B'\cos\phi + B'^2] \quad (7)$$

where the constant K could be evaluated from the various constants entering eqs 1 and 2. Clearly, eq 7 can be put into a frequently used form for the torsion angle dependence of vicinal H–H coupling[5,38-40]

$$^3J_{HH'}(\phi) = A\cos^2\phi + B\cos\phi + C \quad (8)$$

where A, B, and C are theoretically or empirically determined quantities. From eqs 5–7, however, it follows that A, B, and C each depend on θ_1, θ_2, the s character of the hybrid orbitals at C_1 and C_2, and the various overlap integrals. The latter depend on internuclear separations $r(C_1$–$C_2)$ and the effective nuclear charges at the two carbon atoms. In the VB perturbation formulation[39,40] the torsion angle dependence in eq 8 follows from the form of the exchange integral between the vicinal hybrid orbitals.

It is sometimes convenient to assume that the hybrid orbitals at a given carbon have approximately the same hybridization and to relate the s character a^2 to the internal angle θ by means of the expression

$$a^2 = -\cos\theta/(1 - \cos\theta) \quad (9)$$

(26) Cooper, M. A.; Elleman, D. D.; Pearce, C. D.; Manatt, S. L. *J. Chem. Phys.* **1970**, *53*, 2343.
(27) Koster, D. F.; Danti, A. *J. Phys. Chem.* **1965**, *69*, 486.
(28) Albriktsen, P. R.; Cunliffe, A. V.; Harris, R. K. *J. Magn. Reson.* **1970**, *2*, 150.
(29) Bacon, M.; Maciel, G. E. *Mol. Phys.* **1971**, *21*, 257.
(30) Laing, J. W.; Sceats, M. G.; Rice, S. A.; Gavin, R. M. *Chem. Phys. Lett.* **1976**, *41*, 419.
(31) Pople, J. A.; Santry, D. P. *Mol. Phys.* **1964**, *8*, 1.
(32) (a) Pople, J. A.; Santry, D. P. *Mol. Phys.* **1964**, *7*, 269. (b) Pople, J. A.; Santry, D. P. *Mol. Phys.* **1965**, *9*, 301.
(33) Pople, J. A.; Santry, D. P. *Mol. Phys.* **1965**, *9*, 311.
(34) Murrell, J. N.; Gil, V. M. S. *Theor. Chim. Acta* **1966**, *4*, 114.
(35) Klessinger, M.; Barfield, M. In *Modelling of Structure and Properties of Molecules*; Maksic, Z. B., Ed.; Ellis Horwood: Chichester, U.K., 1987; pp 269–84.
(36) Pauling, L. *The Nature of the Chemical Bond*, 3rd ed.; Cornell University Press: Ithaca, NY, 1960; Chapter 4.
(37) Mulliken, R. S.; Rieke, C. A.; Orloff, D.; Orloff, H. *J. Chem. Phys.* **1949**, *17*, 1248.
(38) The electronic factors associated with the torsional angle dependence of $^3J_{HH'}$ were given in terms of a valence-bond bond order analysis.[39]
(39) Barfield, M.; Karplus, M. *J. Am. Chem. Soc.* **1969**, *91*, 1.
(40) Barfield, M.; Grant, D. M. *Adv. Magn. Reson.* **1965**, *1*, 149.

Substitution of eq 9 into eq 5 leads to an expression for the overlap integral between hybrid orbitals where

$$A' = [(1 + \cos\theta_1)(1 + \cos\theta_2)]^{1/2} S_{xx} \quad (10a)$$

$$B' = [(1 - \cos\theta_1)(1 - \cos\theta_2)]^{-1/2}\{(\cos\theta_1\cos\theta_2)S_{\sigma\sigma} + (\cos\theta_1\cos\theta_2)^{1/2}S_{ss} + [\cos\theta_2(-\cos\theta_1)^{1/2} + \cos\theta_1(-\cos\theta_2)^{1/2}]S_{s\sigma}\} \quad (10b)$$

in eq 6. Equations 10a,b have the correct limiting forms: For $\theta_1 = \theta_2 = 90°$, B' vanishes and A' is simply the overlap integral S_{xx} between $2p_x$ atomic orbitals perpendicular to the C–C bond direction. For $\theta_1 = \theta_2 = 180°$, $A' = 0$ and B' denotes the overlap between sp hybrids along the bond direction but pointing away from one another such as the C–H bonds in acetylene.

Since this treatment is equivalent to the one of Pople and Santry,[33] it leads to the same coupling constant results. The difference is that an explicit expression for the spin–spin coupling constant in terms of the dihedral angle and the two internal angles is obtained on substituting eqs 10a and 10b into eq 7. Moreover, the resulting equation is of the form of eq 8 except that the θ dependence of the coefficients A, B, and C is now specified. For ethane and ethylene the results are only about two-thirds of the experimental values, but numerical agreement is not expected in view of the approximations which are implicit in eq 2. Somewhat better results were obtained by Murrell and Gil[34] using an analogous perturbation analysis which included off-diagonal elements associated with hybrid carbon orbitals and 1s orbitals of the hydrogen atoms. They concluded that β_{12} dominated the dependence on dihedral angle but the additional integrals played a role in the cis/trans ratio, i.e., the B term of eq 8. These integrals lead to small, additional θ-dependent contributions to A, B, and C but would be much more difficult to obtain analytically.

From eqs 7, 10a, and 10b the vicinal coupling constants can be written in the form

$$^3J_{HH'}(\theta_1,\theta_2,\phi) = c_a\, a(\theta_1,\theta_2)\cos^2\phi + \sum_i c_{bi}\, b_i(\theta_1,\theta_2)\cos\phi + C \quad (11a)$$

where

$$a(\theta_1,\theta_2) = (1 + \cos\theta_1)(1 + \cos\theta_2) \quad (11b)$$

$$b_1(\theta_1,\theta_2) = \cot(\theta_1/2)\cot(\theta_2/2)\cos\theta_1\cos\theta_2 \quad (11c)$$

$$b_2(\theta_1,\theta_2) = \cot(\theta_1/2)\cot(\theta_2/2)(\cos\theta_1\cos\theta_2)^{1/2} \quad (11d)$$

$$b_3(\theta_1,\theta_2) = \cot(\theta_1/2)\cot(\theta_2/2)[\cos\theta_2(-\cos\theta_1)^{1/2} + \cos\theta_1(-\cos\theta_2)^{1/2}] \quad (11e)$$

The C term is usually small in magnitude when $^3J_{HH'}$ is written in the form of eq 8.[41] From semiempirical VB results for the H–C–C angle dependence of $^3J_{HH'}$ in ethane,[5] it will be shown that any θ dependence in C must be 1 order of magnitude smaller than in the other terms, and so the last term in eq 10a is assumed to be independent of θ_1 and θ_2. In eq 11a the dependence of $^3J_{HH'}$ on C–C internuclear separations occurs in the overlap integrals (eq 9), which are implicit in the coefficients c_a, c_{bi}, and C. Therefore, there will be a set of coefficients for each value of r(C–C). In the spirit of semiempirical MO methods, where the β integrals are determined empirically, these coefficients are to be determined in a least-squares sense from the available experimental data. It is assumed that the trigonometric forms of the coefficients in eq 8 are dominated by β_{12} and that other integrals will have the effect of slightly modifying the empirically determined coefficients.

The term containing $\cos^2\phi$ (the A term) in eq 11a is the most important term controlling the vicinal coupling constants. The θ dependence is relatively simple when compared with the $\cos\phi$ term. Because the latter is negative for $90° < \theta < 180°$, eq 11e is opposite in sign to eqs 11c and 11d and the summation in eq 11a is the small difference between large terms of opposite signs.

The VB results for the θ dependence of $^3J_{HH'}$ in an ethanic fragment gave numerical estimates corresponding to small deviations $\Delta\theta$ from the tetrahedral values θ_0 of the C–C–H angles.[5] In this limit it is of interest to see if eqs 11a–e and the VB results are consistent.[5] However, before such a comparison can be made, it is necessary to make a trigonometric substitution for $\cos^2\phi$ to get eq 8 into the form involving $\cos(2\phi)$, which was adopted in ref 5

$$^3J_{HH'}(\phi) = (A/2)\cos(2\phi) + B\cos\phi + [C + (A/2)] \quad (12a)$$

where A, B, and C are the constants in eq 8 and the following were based on the numerical VB results for an ethanic fragment

$$A/2 \approx 4.2[1 - 0.024(\Delta\theta_1 + \Delta\theta_2)] \quad (12b)$$

$$B \approx -0.5[1 + 0.1(\Delta\theta_1 + \Delta\theta_2)] \quad (12c)$$

$$C + (A/2) \approx 4.4[1 - 0.027(\Delta\theta_1 + \Delta\theta_2)] \quad (12d)$$

where $\Delta\theta_1$ and $\Delta\theta_2$ are the deviations from the tetrahedral angles at carbons C_1 and C_2. The C term appropriate to eq 11a is the small difference between eqs 12d and 12b, thereby providing partial justification for neglecting the θ dependence of the ϕ-independent term in eq 11a.

Assuming small changes $\Delta\theta$ from the tetrahedral value θ_0, the $\cos\theta$ term which occurs in eq 11b can be expanded about θ_0 to give

$$1 + \cos(\theta_0 + \Delta\theta) = (1 + \cos\theta_0)[1 - (\pi\Delta\theta/180)\tan(\theta_0/2)]$$

For small changes, $\Delta\theta$ from the tetrahedral angle ($\pi\tan(\theta_0/2)/180) = 0.025$ deg^{-1} is the value of the θ dependence as a fraction of the total. This value is in good agreement with the 0.024- and 0.027-deg^{-1} values in eqs 12b and 12d, respectively.[5] Analysis of the B-term θ dependence in eqs 11c–11e is similar, but the results are not directly comparable to eq 12c without specifying the coefficients in eq 11a. In the following sections it will be demonstrated that the θ dependence in the coefficient of the $\cos\phi$ term is more complicated than implied in eq 12c. From eq 11a and the empirical ethanic coupling constant data, for example, it appears that the B term is negative but has a positive slope for θ angles less than about 90°. A disparity should not be surprising because it was previously assumed[5] that $\Delta\theta$ values in eq 12b–d were small.

To determine the coefficients in eq 11a from the coupling constants, the internal angles and the torsion angles must be specified. Molecular mechanics calculations were based on the MMX force field derived from Allinger's MM2 force field[42] in the PCMODEL program.[43] Agreement between these and ab initio results is generally quite good. An important exception occurs for bicyclo[2.2.1]heptene where MMX and ab initio results for the bridgehead protons differ by approximately 4°.[44] This leads to disparities of several degrees in both dihedral angles and internal angles associated with these protons. Since a large fraction of the ethanic data occurs for the bridgehead protons of the bicyclo[2.2.1]heptene framework (see Table I), ab initio MO optimized geometries were used for these cases. All ab initio MO geometries are optimized at the HF/3-21G* or 6-31G** levels using the GAUSSIAN 88[45] computer codes on a CONVEX 220 minisupercomputer. All bond lengths and angles are optimized values subject only to the symmetry constraints implicit in **1**, **2**, **6**, and **7**.

(41) It should be clearly understood that this statement is not necessarily correct if trigonometric substitution into eq 8 is used to put the dependence in the form $^3J_{HH'} = A''\cos(2\phi) + B''\cos\phi + C''$. In this expression C'' has a substantial magnitude because $C'' = C + (A/2)$. In this form it would probably be inappropriate to neglect the internal angle dependence of C''.

(42) (a) Allinger, N. L. *J. Am. Chem. Soc.* **1977**, *99*, 8127. (b) Burkert, U.; Allinger, N. A. *Molecular Mechanics*; American Chemical Society: Washington, DC, 1982.
(43) Gajewski, J. J.; Gilbert, K. E.; McKelvie, J. In *Advances in Molecular Modeling*, Liotta, D., Ed.; JAI Press: Greenwich, CT, 1990; Vol. 2, PCMODEL, Vol. 4.0, Serena Software, Box 3076, Bloomington, IN.
(44) Abraham, R. J.; Fisher, J. *Magn. Reson. Chem.* **1985**, *23*, 856.
(45) GAUSSIAN 88: Frisch, J. M.; Head-Gordon, M.; Schlegel, H. B.; Raghavachari, K.; Binkley, J. S.; Gonzalez, C.; Defrees, D. J.; Fox, D. J.; Whiteside, R. A.; Seeger, R.; Melius, C. F.; Baker, J.; Martin, R. L.; Kahn, L. R.; Stewart, J. J. P.; Fluder, E. M.; Topiol, S.; Pople, J. A. Gaussian, Inc., Pittsburgh, PA.

Results and Discussion

1. Internal Angle Dependence of $^3J_{HH'}$ in Ethanic (CHCH) Systems. Although the literature for ethanic coupling is enormous, there are only a few examples for relatively rigid and unsubstituted molecules. Some of these are used to investigate the importance of internal angles for ethanic coupling via eq 11. Molecules were selected to avoid complexities of conformational averaging, substituent effects, and alternative coupling paths as these would further complicate investigations of the effects of structural changes. In Table I structural data and vicinal coupling constants are given for molecules **1**–**5**, cubane **6**, and cyclopropane **7**. In

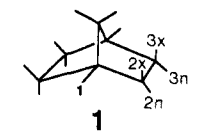

1

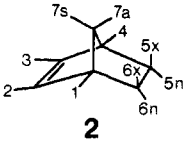

2

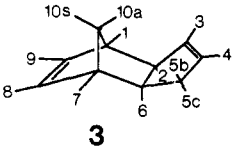

3

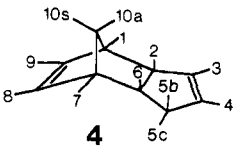

4

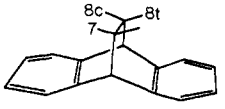

5

the first few columns of Table I are collected the molecular data from optimized ab initio MO results[45] obtained either at the HF/6-31G** or the 3-21G* levels as specified. An exception is **5** for which results were based on MMX optimizations. Included in successive columns of Table I are C–C internuclear distances r(C–C), dihedral angles ϕ, and internal angles θ_1 and θ_2. Note that most of the H–C–C angles in Table I are larger than the tetrahedral angle and several are substantially (6–7°) larger. Experimental vicinal H–H (ethanic) coupling constant data are given in the next to the last column of the table.

All but three of the molecules in Table I have either the bicyclo[2.2.1]heptane **1** or the bicyclo[2.2.1]heptene **2** framework. In **1** the exo–exo coupling constant in the ethylene bridge is several hertz larger than the endo–endo value.[21] However, in the unsaturated molecule **2** the two coupling constants are nearly equal. Semiempirical FPT-INDO (finite perturbation theory in the approximation of intermediate neglect of differential overlap) calculations satisfactorily reproduced these experimental observations with the assumption that the C–C–H angles in the ethane bridge were the same.[21] A series of calculations was performed to investigate qualitatively the relevant electronic factors. Electronic interactions between the methylene bridge and the ethane bridge were shown to provide alternative coupling mechanisms such that ^3J(exo–exo) > ^3J(endo–endo) in **1**. For bicyclo[2.2.1]heptene, however, these two types of coupling are nearly equal because of additional electronic contributions associated with the π-electrons of the ethylene bridge. Since electronic interactions outside the an HC–CH moiety are not implicit in the formulation leading to eq 11, it is not surprising that inclusion of the exo–exo and endo–endo values in the linear regression leads to relatively poor results. There are few reliable experimental data for proton coordinates in multicyclic hydrocarbons. It was hoped that readily implemented, molecular mechanics techniques would be adequate for this purpose. In general, these methods give good agreement with ab initio MO results.[42] The only major exception encountered here involved the internal and dihedral angles associated with the bridghead protons of the bicyclo[2.2.1]heptene system. Unfortunately, many of the entries in Table I involve such protons, and the use of molecular mechanics results (MMX) leads to inconsistencies. For example, the calculated magnitudes of cis and trans cyclopropane coupling constants are reversed.

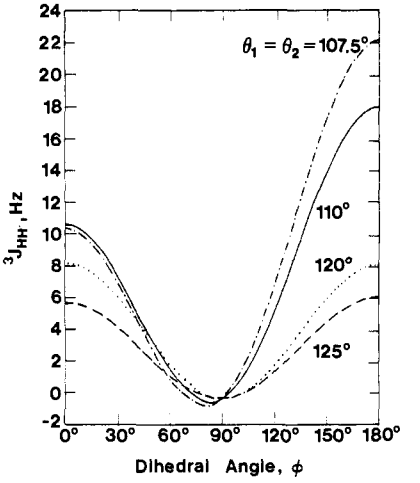

Figure 2. Vicinal H–H coupling constants for an ethanic system (eq 13) plotted as a function of the dihedral angle ϕ for internal H–C–C angles $\theta_1 = \theta_2 = 107.5°$ (dot–dash curve), 110° (solid curve), 120° (dotted line), and 125° (dashed line).

Coefficients in eq 11a were evaluated by linear regression from a subset of 23 data points in Table I excluding the exo–exo and endo–endo coupling constants in the ethane bridges and the cyclopropane data.

$$^3J_{HH'}(\theta_1,\theta_2,\phi) = 33.8\ a(\theta_1,\theta_2)\cos^2\phi + [-1258.4\ b_1(\theta_1,\theta_2) - 650.5\ b_2(\theta_1,\theta_2) - 905.3\ b_3(\theta_1,\theta_2)]\cos\phi - 0.3\ \text{Hz} \quad (13)$$

The correlation coefficient r^2 is 0.974, and the standard deviation is 0.5 Hz. Data from eq 13 are entered in the sixth column of Table I for comparison with the experimental data in the seventh column. Differences between the experimental results and those of eq 13 are given in the last column. The exo–exo and endo–endo coupling constants from eq 13 are 10.6 and 10.4 Hz, respectively. This small difference arises because the internal angles for endo protons are about 2° greater than for exo protons. The 1–2-Hz differences with the experimental data are qualitatively consistent with the MO observations in which the interactions between the bridges were eliminated.[21]

It was of interest to investigate the applicability of MMX molecular mechanics structural data for ethanic coupling. Values obtained from eq 13 with MMX optimized angular data are given in parentheses in Table I. Not surprisingly, the largest disparities (ca. 1.3 Hz) occur for certain bridgehead protons as these have the greatest geometrical differences.

Although cubane has, by far, the largest C–C–H angle in this series, the agreement is good. Even better, perhaps, are the results within 0.4 Hz or less for both the cis and trans coupling constants in cyclopropane which were not included in the linear regression analysis. It should be noted that the 144° dihedral angle for the trans coupling is an isolated example and corresponds to a relatively inaccessible region for rigid molecules. In fact, there are only a few examples of coupling situations in Table I for which dihedral angles are greater than 65°.

The importance of the θ dependence of vicinal coupling constants in ethanic fragments is depicted in Figure 2 where $^3J_{HH'}(\theta_1,\theta_2,\phi)$ data from eq 13 are plotted versus ϕ for representative $\theta_1 = \theta_2$ values (107.5, 110, 120, 125°). The predicted range of $^3J_{HH'}$ values is greatest for $\phi = 180°$, drops off to negligible differences near 90°, and then stays relatively constant between 40 and 100°. Therefore, the θ dependence of the ethanic $^3J_{HH'}$ data is quite different if the dihedral angle is greater or less than 90°. The reason for this behavior should be clear from Figure 3 where the coefficients (A and B) of the $\cos^2\phi$ and the $\cos\phi$ terms are plotted (dashed and solid lines, respectively) as a function of $\theta_1 = \theta_2$. Also plotted (solid and dot–dashed lines, respectively) in Figure 3 are $^3J_{HH'}(\phi = 0°)$ and $^3J_{HH'}(\phi = 180°)$. These are, respectively, the sum ($A + B + C$) and the difference ($A - B + C$) of the A and B terms plus the constant C in eq 13. Since the slopes of A and B are just about equal in magnitude and opposite

Table I. Structural Data and Calculated and Experimental $^3J_{HH'}$, in Ethanic (CHCH) Moieties of a Series of Cyclic Molecules[a]

compound	r(C–C), Å	φ, deg	θ_1, deg	θ_2, deg	$^3J(\phi)$,[b] Hz	$^3J(\theta_1,\theta_2,\phi)$,[c] Hz	J_{expt}, Hz	Δ^3J, Hz
				Bicyclo[2.2.1]heptane[d,e] (**1**)				
2x–3x	1.557	0.0	111.0	111.0	9.0	10.6 (11.2)	12.2	−1.6[f]
2n–3n	1.557	0.0	112.8	112.8	9.0	10.4 (11.1)	9.1	1.3[f]
2x–3n	1.557	120.3	111.0	112.8	4.3	4.2 (5.2)	4.6	−0.4
				Bicyclo[2.2.1]heptene[d,e] (**2**)				
1–6n	1.557	76.3	112.2	110.4	0.4	−0.2 (0.7)	0.6	−0.8
1–6x	1.557	43.9	112.2	111.9	4.3	4.8 (5.8)	3.7	1.2
1–7s	1.539	62.7	117.3	113.7	1.6	1.7 (2.8)	1.8	−0.1
1–7a	1.539	63.0	117.3	113.4	1.6	1.6 (1.7)	1.5	0.1
5x–6x	1.551	0.0	111.2	111.2	9.0	10.4 (11.1)	9.4	1.0[f]
5n–6n	1.551	0.0	113.0	113.0	9.0	10.6 (11.2)	9.0	1.6[f]
5x–6n	1.551	121.0	113.0	111.2	4.4	4.3 (5.3)	3.9	0.4
				exo-Tricyclo[5.2.1.$0^{2,6}$]deca-3,8-diene[g] (**3**)				
1–10a	1.550	62.3	117.4	113.2	1.6	1.8 (1.9)	1.5	0.3
1–10s	1.550	65.1	117.4	112.3	1.4	1.5 (2.8)	1.7	−0.2
5b–6	1.560	3.4	111.4	111.5	9.0	10.5 (10.1)	10.8	−0.3
5c–6	1.560	116.8	111.0	111.5	3.6	3.6 (3.6)	3.1	0.5
7–10s	1.552	64.1	117.5	112.3	1.4	1.6 (2.1)	1.7	−0.2
7–10a	1.552	62.7	117.5	113.6	1.6	1.7 (1.0)	1.5	0.2
2–6	1.575	0.2	113.3	112.3	9.0	10.4 (10.2)	8.2	2.2[f]
				endo-Tricyclo[5.2.1.$0^{2,6}$]deca-3,8-diene[g] (**4**)				
1–10a	1.555	62.9	117.4	113.2	1.6	1.6 (1.7)	1.4	0.2
1–10s	1.555	63.6	117.4	112.3	1.5	1.6 (2.0)	1.8	−0.2
5b–6	1.557	2.2	111.4	110.9	9.0	10.6 (11.2)	9.6	1.0
5c–6	1.557	118.5	111.8	110.9	3.9	4.1 (4.4)	4.0	0.1
7–10s	1.555	63.6	117.2	112.7	1.5	1.6 (2.9)	1.8	−0.2
7–10a	1.555	63.0	117.2	113.2	1.6	1.6 (1.7)	1.4	0.2
1–2	1.573	42.9	111.1	109.3	4.6	5.0 (5.7)	4.0	1.0
6–7	1.568	43.8	109.4	111.9	4.4	4.8 (5.7)	4.0	0.8
2–6	1.571	0.3	112.1	111.0	9.0	10.6 (11.2)	8.0	2.6[f]
				Dibenzocyclooctadiene[h] (**5**)				
7–8cis	1.550	0	110.3	110.3	9.0	10.6 (11.3)	11.1[i]	−0.5
7–8trans	1.550	118	110.3	110.3	3.8	4.5 (5.1)	4.4[i]	0.1
				Cubane[e] (**6**)				
	1.559	0	125.3	125.3	9.0	5.5 (6.2)	5.3[j]	0.2
				Cyclopropane[e] (**7**)				
cis	1.497	0.0	118.1	118.1	9.0	9.0 (10.1)	9.0[h]	0.0
trans	1.497	144.1	118.1	118.1	9.4	6.0 (7.3)	5.6[h]	0.4

[a] Abbreviations: a, anti; s, syn; x, exo; n, endo. [b] $^3J_{HH'}(\phi) = 11.0\cos^2\phi - 2.3\cos\phi + 0.3$ Hz. [c] Results from eq 13. Values in parentheses are obtained from eq 13 with angular data from MMX calculations. [d] Coupling constants from refs 21 and 44. [e] Optimized values at the HF/6-31G** level. [f] Exo–exo and endo–endo vicinal coupling constants. [g] Vicinal coupling constants from: Ramey, K. C.; Lini, D. C. *J. Magn. Reson.* **1970**, *3*, 94. Ab initio optimizations performed at the HF/3-21G* level. [h] Coupling constants taken from: Fay, C. K.; Grutzner, J. B.; Johnson, L. F.; Sternhell, S.; Westerman, P. W. *J. Org. Chem.* **1973**, *38*, 3122. [i] MMX optimization.[43b] [j] This is the typical $^3J_{HH'}$ value cited for substituted cubanes in ref 20.

in sign for H–C–C angles less than about 115° in Figure 3, the curve for $^3J_{HH'}(\phi = 0°)$ has a shallow maximum near the tetrahedral angle. As a consequence, $^3J_{HH'}(\phi = 0°)$ varies by only a few hertz even for very large changes of internal angles. Even smaller variations occur for dihedral angles in the range $0° < \phi < 90°$ in Figure 2. For trans ethanic coupling, the *A* and *B* terms reinforce one another and the slope is just about twice the slope for *A* in Figure 3. Since most of the data in Table I correspond to dihedral angles less than 90°, these results provide a rationale for the usual neglect of internal angle changes in most strained multicyclic systems. Ethanic coupling constants having little sensitivity to changes of internal angles are at variance with the VB results in eqs 12a–d. These indicated that ethanic coupling constants should vary by −0.27 Hz deg^{-1} for each C–C–H angle. Thus, for dihedral angles of 0° and 180° with both internal angles 5° greater than tetrahedral, the VB results suggest that vicinal H–H coupling should be decreased by 2.7 and 1.7 Hz, respectively. However, from eq 13 a 5° increase in internal angles should decrease these coupling constants by 0.0 and 6.8 Hz, respectively.

Linear regression among the same set of 23 data points in Table II with complete neglect of the θ dependence leads to the expression

$$^3J_{HH'}(\phi) = 11.0\cos^2\phi - 2.3\cos\phi + 0.3 \qquad (14)$$

where the correlation coefficient r^2 is 0.877 and the standard

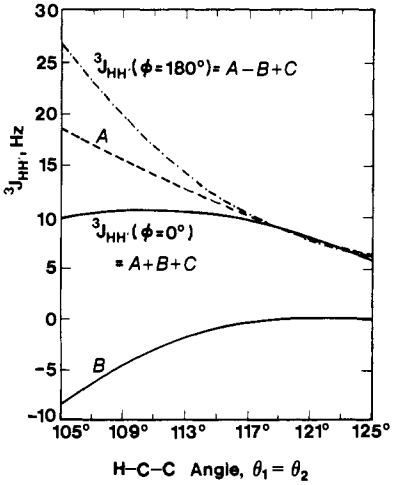

Figure 3. Plot of the coefficients *A* and *B* (dashed and solid lines) in the expression for ethanic $^3J_{HH'}$ (eq 13) as a function of the H–C–C angles $\theta_1 = \theta_2$. Also plotted (solid and dot–dash lines, respectively) are $^3J_{HH'}(\phi = 0°)$ and $^3J_{HH'}(\phi = 180°)$ corresponding to the sum $(A + B + C)$ and the difference $(A - B + C)$ of the *A* and *B* terms plus the constant *C* in eq 8 or eq 13.

Table II. Structural Data based on Calculated MMX and Experimental Data for Vicinal H–H Coupling in Ethylenic (CH=CH) Fragments of Cyclic and Acyclic Monoenes and Dienes[a]

compound	r(C–C), Å	ϕ, deg	$\theta_1 = \theta_2$, deg	$^3J(\theta_1,\theta_2,\phi)$,[b] Hz	J_{expt}, Hz	Δ^3J, Hz
cyclopropene (**8**)	1.276	0	149.3	−0.5	±1.3[c]	
cyclobutene (**9**)	1.339	0	133.8	2.6	2.9[d]	−0.3
bicyclo[2.2.1]heptadiene (**10**)	1.341	0	127.2	5.5	5.3[e]	0.2
benzobicyclo[2.2.1]heptene (**12**)	1.342	0	126.1	5.9	5.4[f]	0.5
cyclopentene (**13**)	1.337	0	124.9	6.7	5.6[g]	1.1
bicyclo[2.2.1]heptene (**2**)	1.338	0	127.3	5.5	5.8[e]	−0.3
5,8-dimethoxy-1,4-dihydro-1,4-ethanonaphthalene (**14**)	1.341	0	122.8	7.7	7.6[h]	0.1
benzobicyclo[2.2.2]octadiene (**15**)	1.342	0	122.7	7.7	7.8[i]	−0.1
bicyclo[2.2.2]octene (**16**)	1.339	0	123.6	7.4	8.2[g]	−0.8
cyclohexene (**17**)	1.341	0	119.4	9.7	10.1[g,j]	−0.4
cyclooctene (**18**)	1.340	0	116.7	11.2	10.4[g]	0.8
cis-2-butene (**19**)	1.343	0	117.7	10.7	10.9[k]	−0.2
cycloheptene (**20**)	1.340	0	118.4	10.3	11.0[g]	−0.7
cis-di-*tert*-butylethylene (**21**)	1.353	1	111.0	14.2	14.2[g]	0.0
trans-2-butene (**22**)	1.342	180	119.5	15.3	15.1[k]	0.2
trans-di-*tert*-butylethylene (**23**)	1.343	180	118.6	15.9	16.1[g]	−0.2

[a] If H–C–C angles are not included, $^3J_{HH'}(\phi) = 11.9 - 3.7 \cos\phi$, corresponding to cis and trans coupling constants of 8.1 and 15.6 Hz, respectively. [b] Equation 15. [c] Lambert, J. B.; Jovanovich, A. P.; Oliver, Jr., W. L. *J. Phys. Chem.* **1970**, *74*, 2221. [d] Hill, E. A.; Roberts, J. D. *J. Am. Chem. Soc.* **1967**, *89*, 2047. [e] Garbisch, E. W., Jr. *Chem. Commun.* **1968**, 332. [f] Tori, F.; Muneyuki, R.; Tanida, H. *Can. J. Chem.* **1963**, *41*, 3142. [g] Reference 7d. [h] The preparation and chemical shifts are given by: Smith, W. B.; Stock, L.; Cornforth, S. J. *Tetrahedron* **1983**, *39*, 1379. The coupling constants were obtained here using spin decoupling and computer spin simulations. [i] Tori, K.; Takano, Y.; Kitahonoki, K. *Chem. Ber.* **1964**, *97*, 2798. [j] Auf der Heyde, W.; Lüttke, W. *Chem. Ber.* **1978**, *111*, 2384. [k] Harris, R. K. and Howes, B. R. *J. Mol. Spectrosc.* **1968**, *28*, 191.

deviation is 1.1 Hz. Values of $^3J_{HH'}(\phi)$ from eq 14 are tabulated in the sixth column of Table I. Of course deviations are somewhat larger than those based on eq 13. However, the only substantial disparities occur for dihedral angles greater than 90° and for cubane which has θ angles about 16° greater than tetrahedral. Equation 14 gives a value of 9.0 Hz for $\phi = 0°$ in comparison with an experimental value close to 5.3 Hz in substituted cubanes.[20] A similar disparity is noted for the trans ($\phi = 144°$) coupling in cyclopropane even though the internal angles are only about 9° greater than the tetrahedral values.

2. Internal Angle Dependence of $^3J_{HH'}$ in Ethylenic (CH=CH) Systems. Since the internal angles for nominally sp^2-hybridized carbons in unsaturated molecules have an even larger range than those for saturated hydrocarbons in Table I, these provide an excellent demonstration of the applicability of the proposed θ dependence of $^3J_{HH'}$. Entries in Table II are given in order of increasing H–H coupling constants in the next to the last column of Table II. The first 14 entries correspond to the cis arrangement of the H atoms about the C=C double bond. These are plotted in Figure 4 as a function of $\theta_1 = \theta_2$. As the H–C–C angles decrease from 149 to 111°, the cis coupling constants increase from 1.3 to 14 Hz. This increase of the $^3J_{HH'}$(cis) in these cyclic molecules follows closely the form of the A coefficient in eq 11a. The only coupling constant data for trans arrangements are those for *trans*-2-butene and *trans*-di-*tert*-butylethylene. Molecular mechanics values for $r(C_1–C_2)$ and $\theta_1 = \theta_2$ are given in the second and third columns, respectively, of Table II.

The coefficients in eq 11a were evaluated by linear regression of all data in Table II except cyclopropene

$$^3J_{HH'}(\theta_1,\theta_2,\phi) = 41.1\ a(\theta_1,\theta_2)\cos^2\phi + [-752.8\ b_1(\theta_1,\theta_2) - 406.0\ b_2(\theta_1,\theta_2) - 541.6\ b_3(\theta_1,\theta_2)]\cos\phi + 1.9\ \text{Hz} \quad (15)$$

where the correlation coefficient r^2 is 0.982 and the standard deviation is 0.6 Hz. For comparison, the data obtained from eq 15 are entered in the fifth column of Table II and the differences from the experimental values are given in the last column. To examine their relative importance, the coefficients (A and B) of $\cos^2\phi$ and $\cos\phi$ terms in eq 15 are plotted in Figure 4 (solid lines) as a function of $\theta_1 = \theta_2$. The total $^3J_{HH'}(\theta_1 = \theta_2, 0°)$ from eq 15 is given by the dashed line in the figure. For internal angles greater than about 110°, the B term is relatively flat and the A term dominates the internal angle dependence of the vicinal coupling. Also included in the figure are the experimental cis $^3J_{HH'}$ values from Table II (these are given by the filled circles in Figure 4) and the semiempirical VB results for cis H–H coupling in an ethylenic fragment at $\theta = 110$, 120, and 130° (open squares). For

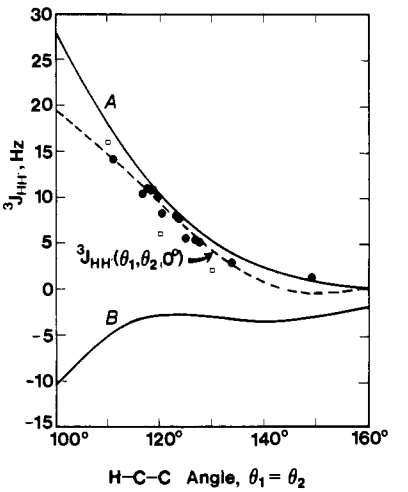

Figure 4. Plot of the coefficients A and B (solid lines) in the expression for ethylenic $^3J_{HH'}$ (eq 15) as a function of the H–C–C angles $\theta_1 = \theta_2$. Also plotted (dashed line) is $^3J_{HH'}(\theta_1,\theta_2,\phi)$: (●) experimental from Table II; (□) semiempirical VB.[5]

H–C–C angles as large as 150° for cyclopropene, the A term nearly vanishes and could become smaller in magnitude than the B term. In this situation, the vicinal coupling in cyclopropene could be negative but the sign seems not to have been measured. The value plotted in Figure 4 is the positive one. Other reasons for excluding cyclopropene from the linear regression are the much shorter C–C bond length and the possibility of long-range contributions over four saturated bonds.[46] In the absence of θ-dependent terms in eq 15, the $^3J_{HH'}$ data for $\phi = 0°$ in Figure 4 would all have the same value.

3. Internal Angle Dependence of $^3J_{HH'}$ in Allylic (C=CHCH) Systems. The conformational dependence of this type of vicinal H–H coupling was described by Garbisch[24] who noted that angularly dependent π-electron contributions should also be included for this type of coupling. Because this indirect effect involves a σ–π mechanism,[47] the dependence on dihedral angle has the form $a'\sin^2\phi + b' = -a'\cos^2\phi + (a' + b')$. Since b' is usually small and a' is typically about 2 Hz, the magnitude of c_a and C in eq 12 should be decreased and increased proportionally from the ethanic values, respectively.[48]

(46) Barfield, M.; Chakrabarti, B. *Chem. Rev.* **1969**, *69*, 757.
(47) Karplus, M. *J. Chem. Phys.* **1960**, *33*, 1842.

Table III. Structural Data and Experimental and Calculated $^3J_{HH'}$ in Allylic (C=CHCH) Moieties of a Series of Cyclic, Unsaturated Molecules

compound	r(C–C), Å	φ, deg	θ_1, deg	θ_2, deg	$^3J(\phi)$,[a] Hz	$^3J(\theta_1,\theta_2,\phi)$,[b] Hz	J_{expt}, Hz	Δ^3J, Hz
cyclobutene (**9**)	1.515	65	112.4	131.9	1.0	1.0	1.0[c]	0.0
bicyclo[2.2.1]heptadiene (**10**)	1.512	21	118.4	125.2	4.0	2.9	2.9[d]	0.0
exo-tricyclo[5.2.1.$0^{2,6}$]deca-3,8-diene[e] (**3**)								
4 – 5c	1.502	59	111.3	122.0	1.3	2.1	2.0	0.1
4 – 5b	1.502	61	111.0	122.0	1.2	1.9	2.0	–0.1
benzobicyclo[2.2.1]heptene (**12**)	1.514	22	117.9	125.8	3.9	3.0	3.0[f]	0.0
benzobicyclo[2.2.2]octene (**24**)	1.511	3	112.3	122.5	4.7	6.1	6.1[g]	0.0
5,8-dimethoxy-1,4-dihydro-1,4-ethanonaphthalene (**14**)	1.511	2	111.6	122.6	4.7	6.2	6.2[h]	0.0
1,1-dimethyl-3,3-di-*tert*-butylpropene (**25**)	1.516	172	107.9	114.5	11.3	11.6	11.6[i]	0.0
cyclopropene (**8**)	1.474	73	120.2	147.3	0.8	0.4	±1.8[j]	
cyclopentadiene (**26**)	1.508	62	111.3	124.0	1.1	1.7	1.3[k]	0.4
cyclopentene (**13**)	1.503	46	111.9	123.1	2.1	3.0		
					1.5		2.1	2.1[l] 0.0
	1.503	76	109.2	123.1	0.8	1.2		

[a] $^3J_{HH'}(\phi) = 6.9\cos^2\phi - 3.4\cos\phi + 1.2$ Hz. [b] Equation 17. [c] Footnote *d* of Table II. [d] Footnote *e* of Table II. [e] Footnote *g* of Table I. [f] Parameters, which were provided by Dr. D. E. Minter, were obtained by the methods described by: Minter, D. E.; Marchand, A. P.; Lu, S.-P. *Magn. Reson. Chem.* **1990**, *28*, 623. [g] Footnote *i* of Table II. [h] Footnote *h* of Table II. [i] Bothner-By, A. A.; Naar-Colin, C.; Günther, H. *J. Am. Chem. Soc.* **1962**, *84*, 2748. [j] Footnote *c* of Table II. [k] Reference 26. [l] Reference 7d.

Table IV. Structural Data and Calculated and Experimental Data for Vicinal H–H Coupling in Diene (C=CHCH=C) Moieties of Cyclic and Acyclic Polyenes

compound	r(C–C), Å	φ, deg	θ_1, deg	θ_2, deg	$^3J(\phi)$,[a] Hz	$^3J(\theta_1,\theta_2,\phi)$,[b] Hz	J_{expt}, Hz	Δ^3J, Hz
cyclopentadiene (**26**)	1.474	0	125.8	125.8	4.6	1.8	1.9[c]	–0.1
cyclohexadiene (**27**)	1.469	7	120.1	119.4	4.6	5.4	5.1[c]	0.3
dicyanonorcaradiene (**28**)	1.466	0	119.2	119.2	4.6	5.8	6.2[d]	–0.4
cycloheptatriene (**29**)	1.467	34	116.6	117.4	4.4	5.4	5.5[e]	–0.1
cyclooctatetraene (**30**)	1.492	61	117.4	117.4	4.3	3.7	3.9[f]	–0.2
trans-butadiene (**31**)	1.470	180	119.3	119.3	10.7	10.8	10.4[g]	0.4
cis-pentadiene (**32**)	1.472	179	120.9	117.6	10.7	10.7	11.0[g,h]	–0.2
trans-pentadiene (**33**)	1.471	180	119.5	118.9	10.7	10.8	10.3[g,h]	0.5
cis,cis-hexadiene (**34**)	1.473	180	118.5	118.5	10.7	10.9	11.4[g,h]	–0.5
cis,trans-hexadiene (**35**)	1.473	180	120.4	117.2	10.7	10.8	10.9[h]	–0.1
trans,trans-hexadiene (**36**)	1.473	180	119.0	119.0	10.7	10.8	10.3[h]	0.5

[a] $^3J_{HH'}(\phi) = 2.5\cos^2\phi - 3.0\cos\phi + 5.2$ Hz. [b] Equation 18. [c] Reference 26. [d] Ganter, C.; Roberts, J. D. *J. Am. Chem. Soc.* **1966**, *88*, 741. [e] Günther, H.; Wenzl, R. *Z. Naturforsch.* **1967**, *B22*, 389. [f] Larson, W. D.; Anet, F. A. L. Unpublished results cited by Cooper et al.[26] [g] Reference 29. [h] Reference 28.

Since $r(C_1C_2=)$ values in Table III are about 0.16 Å greater than for $r(C_1=C_2)$, the magnitude of the c_a coefficient should be even further reduced from the ethanic value in eq 13. A number of $^3J_{HH'}$ values for a series of cyclic monoenes, dienes, and 1,1-dimethyl-3,3-di-*tert*-butylpropene (**25**) are given in the next to the last column of Table III. These correspond to situations in which the C_1 and C_2 carbons are, respectively, sp^2 and sp^3 hybridized. Also entered in Table III are bond lengths $r(C_1–C_2)$, dihedral angles φ, and internal angles θ_1 and θ_2, all based on MMX results (PCMODEL). Dihedral angles are only reported to the nearest degree as these typically vary by 0.5° in successive runs or in situations where they should be the same from considerations of symmetry. Except for **25**, which provides the only information for a trans arrangement, internal angles are greater than trigonal and tetrahedral.

A linear regression analysis was performed for all data in Table III except cyclopropene, cyclopentadiene, and cyclopentene

$$^3J_{HH'}(\theta_1,\theta_2,\phi) = 23.8\,a(\theta_1,\theta_2)\cos^2\phi + [-183.0\,b_1(\theta_1,\theta_2) - 21.7\,b_2(\theta_1,\theta_2) - 67.9\,b_3(\theta_1,\theta_2)]\cos\phi + 1.2\text{ Hz} \quad (16)$$

where $r^2 = 0.9998$ and the standard deviation is 0.1 Hz. Data from eq 17, which are included in the seventh column of Table III, compare very well with the experimental coupling constant data as measured by the differences between calculated and experimental results in the last column of the table.

Cyclopropene and cyclopentadiene were not included in the regression analysis leading to eq 16 because each of these has a nonnegligible, alternative coupling path which is not implicit in eq 11a. The vicinal coupling in cyclopropene has an additional four-bond allylic path which is estimated to contribute about –3 Hz for the 73° dihedral angle assuming the applicability of an equation developed for less strained molecular situations.[46] As a consequence, it seems likely that the experimental value of 1.8 Hz should have a negative sign in Table III. Similarly, cyclopentadiene has an alternative, six-bond path over the conjugated π-electron system. From semiempirical VB calculations[46] this is estimated to be –0.6 Hz which partially offsets the disparity of 0.4 Hz in Table III. Assuming that $^3J_{HH'}$ in cyclopentene is an average of the vicinal coupling to the two protons of the methylene group, (3.0 + 1.2)/2 = 2.1 Hz, which is in excellent agreement with the 2.1-Hz experimental value.

Linear regression among the same set of nine data points in Table III, with complete neglect of the θ dependence, leads to the expression

$$^3J_{HH'}(\phi) = 6.9\cos^2\phi - 3.4\cos\phi + 1.2\text{ Hz} \quad (17)$$

Values of $^3J_{HH'}$ from eq 17 are tabulated in the sixth column of Table I. The deviations are not great in comparison to those based on eq 16: The neglect of the internal angles leads to errors no greater than 1.7 Hz in Table III. The reason for the small differences is that the vicinal coupling constant data are in a range of φ and/or θ angles for which the internal angle dependence is not so important. It is important to note, however, that a θ-dependent *B* term is necessary to account for the 3-Hz difference in the experimental values for φ = 0° and 22° in Table III.

4. Internal Angle Dependence of $^3J_{HH'}$ in Diene (C=CHCH=C) Systems. Entered in Table IV are molecular mechanics data for $r(C_1–C_2)$, dihedral angles φ, and the internal angles θ_1 and θ_2 for a series of cyclic and acyclic polyenes. Except for cyclopentadiene, the internal angles are close to the trigonal values. Experimental $^3J_{HH'}$ data are given in the next to the last column of Table IV. The coefficients in eq 11a were obtained by linear

(48) It is here assumed that the θ dependence of the π-electron contributions is small and can be reasonably accommodated into the trigonometric form of eqs 11a–c.

regression from all 11 entries in the table

$$^3J_{HH'}(\theta_1,\theta_2,\phi) = 17.5\ a(\theta_1,\theta_2)\cos^2\phi + [-1949\ b(\theta_1,\theta_2) - 883.3\ b_2(\theta_1,\theta_2) - 1302\ b_3(\theta_1,\theta_2)]\cos\phi + 3.7\ \text{Hz} \quad (18)$$

where r^2 is 0.989 and the standard deviation is 0.4 Hz. Data from eq 18 and the experimental data are entered in the seventh and eight columns, respectively. Although the number of distinct data points is only slightly larger than the number of parameters and the range of internal angles is substantially smaller here than for the ethylenic situations in Table II, the monotonic decrease of $^3J_{HH'}$ with increasing internal angle is similar. No clear trends are evident in the data for butadiene and the methyl-substituted butadienes in Table IV. In these cases it is usually assumed that conformational averaging about the C-C single bond is not a factor. Variations of $^3J_{HH'}$ have been attributed to a splaying of the C—C=C angles and a concomitant compression of the C=C—H angles.[28,29] This type of analysis was extended to *all-trans*-retinal and 11-*cis*-retinal.[30] Unfortunately, the spread in the vicinal H-H coupling constant values in Table IV is about the same order of magnitude as the errors in the computed values so no conclusions can be drawn in this regard.

Linear regression among the data in Table IV, with complete neglect of the θ dependence leads to the expression

$$^3J_{HH'}(\phi) = 2.5\cos^2\phi - 3.0\cos\phi + 5.2\ \text{Hz} \quad (19)$$

Values of $^3J_{HH'}$ from eq 19 are tabulated in the sixth column of Table I. The constancy of these values clearly indicates the importance of internal angle variations for this type of coupling.

Conclusions

An analytic expression for $^3J_{HH'}$ is derived and presented here to describe the dependence of vicinal H-H coupling on the internal angles θ_1 and θ_2 as well as the torsion angle ϕ. Although this study has emphasized interproton coupling, the formalism is quite generally applicable to other type of vicinal coupling constants. The dependencies on C-C internuclear distance appear in the coefficients of the trigonometric terms. With empirical criteria for these coefficients and angular data from ab initio MO and molecular mechanics optimized structures, the resulting equations describe all types of vicinal H-H coupling, e.g., coupling in ethanic (CHCH), ethylenic (CH=CH), allylic (C=CHCH), and diene (C=CHCH=C) moieties.

The accurate specification of the vicinal H-H coupling constants in the various moieties will require more experimental data in rigid, unsubstituted molecules. Nevertheless, from this study it is now clear that vicinal coupling constants are functions of both torsion angles and internal angles. In some cases the internal angle dependence is controlled by the coefficient of the $\cos^2\phi$ term in eq 11a which drops off monotonically. An exception is coupling in ethanic fragments having dihedral angles less than 90° because of effective cancellation between the *A* and *B* terms in this range. The coefficients of $\cos^2\phi$ and $\cos\phi$ have almost equal slopes and effectively cancel for dihedral angles less than 90°. Thus, the usual neglect of the internal angle for ethanic coupling seems to be justified for many common situations in relatively rigid multicyclic compounds. However, for dihedral angles greater than 90° the coefficients reinforce one another, thereby leading to very large variations with internal angles.

The very important role of substituents and their orientations has not been addressed in this study. Clearly, substantial changes are expected by both substituent electronic effects and substituent-induced geometry changes. Because of the balance in the *B* term between large terms of opposite sign, it seems likely that any electronic changes such as by electronegative substituents could easily lead to a substantial change in the form of the θ dependence of *B*.

Acknowledgment. Appreciation is expressed to the National Science Foundation for a Chemical Instrumentation Grant to assist in purchasing a CONVEX 220 computer.

Molecular Dynamics of the Primary Photochemical Event in Rhodopsin

Jack R. Tallent, Elaine W. Hyde, Leonore A. Findsen, Geoffrey C. Fox, and Robert R. Birge*

Contribution from the Department of Chemistry, the Center for Molecular Electronics, and the Northeast Parallel Architecture Center, Syracuse University, Syracuse, New York 13244-4100.
Received August 2, 1991

Abstract: The ground-state and excited-state surfaces connecting rhodopsin (R) and bathorhodopsin (B) along the $\phi_{11,12}$ dihedral reaction path were partially adiabatically mapped on the basis of a revised model of the protein binding site with a glutamic acid counterion interacting with the C_{13}-C_{15} region of the chromophore. The ground-state surface was generated by using MNDO/AM1 procedures, and the excited-state surface was generated by using INDO-PSDCI procedures including both single- and double-configuration interaction. The first excited singlet state exhibits a barrierless reaction path for C_{11}=C_{12} dihedral torsion with a local minimum (activated complex) centered at $\phi_{11,12} = 90°$. Semiempirical molecular dynamics procedures are used to simulate the forward and reverse photochemistry. The activated complex is reached in ~375 fs following excitation. The quantum yields (Φ) and the product formation times (t) are calculated on the basis of three semiclassical coupling models. Best results are obtained by including both dynamic and phased (partitioned) nonadiabatic coupling (experimental values): $\Phi_{R\to B} = 0.698$ (0.67); $t_{R\to B} = 1.360$ (~3)ps; $\Phi_{B\to R} = 0.521$ (0.53); $t_{B\to R} = 1.628$ (~3) ps. The nonadiabatic coupling term changes sign at $\phi_{11,12} \cong 92°$ and preferentially enhances $\Phi_{R\to B}$ relative to $\Phi_{B\to R}$. The lower quantum yield of the B → R photoisomerization is also due to the rapid arrival of the trajectory into the activated complex which precludes equilibration of the excited state prior to arrival at the activated complex and lowers the dynamic coupling term. The $S_n \leftarrow S_1$ excited singlet state spectrum is calculated as a function of time following excitation of R. The key feature of the early time spectra (0-325 fs) is the presence of a strong absorption centered between 540 and 580 nm, which is surprisingly similar in oscillator strength and energy to the λ_{max} absorption band of bathorhodopsin. This feature broadens and decreases in intensity once the molecule enters the activated complex. A longer wavelength band at ~780 nm appears after ~375 fs which is diagnostic of C_{11}=C_{12} dihedral angles in the region $80° < \phi_{11,12} < 100°$. A strong $S_n \leftarrow S_1$ absorption band is calculated at ~340 nm, which is relatively insensitive in both location and intensity to changes in the C_{11}=C_{12} dihedral angle.

Rhodopsin (MW ≅ 40 000) is the protein responsible for generating an optic nerve impulse in the visual receptors of the three phyla that possess image-resolving eyes: mollusks, arthropods, and vertebrates.[1,2] The primary sequence[3,4] and presumed

0002-7863/92/1514-1581$03.00/0 © 1992 American Chemical Society